Periodic buckling of smectic-*A* tubular filaments in an isotropic phase

Masayoshi Todorokihara, Yosuke Iwata, and Hiroyoshi Naito*
Department of Physics and Electronics, Osaka Prefecture University, 1-1 Gakuen-cho, Sakai, Osaka 599-8531, Japan
(Received 28 January 2003; published 13 August 2004)

Periodic buckling of smectic-*A* tubular filaments in an isotropic phase has been investigated both experimentally and theoretically in the binary mixture of octyloxycyanobiphenyl and dodecyl alcohol. As the mixture is cooled, straight filaments become unstable and continuously buckle by elongating at a constant periodicity. An analytical solution to the minimization of the curvature elastic energy of the smectic-*A* filament has been shown, and is consistent with the shapes of the buckled filaments. In addition, the dependence of the load on the length of the filament has been numerically calculated, and the critical buckling load of the smectic-*A* filament has been found to be of the order of 1 pN.

DOI: 10.1103/PhysRevE.70.021701 PACS number(s): 61.30.Cz, 02.40.Hw, 46.32.+x, 62.20.Fe

I. INTRODUCTION

A smectic-*A* phase exhibits a variety of spatial patterns during its growth process from an isotropic phase [1–8]. One of the most interesting examples of the processes is the formation of smectic-*A* filamentally structures and their thermotemporal evolution [4–7]. These filaments have a tubular structure (a cylindrical structure with an isotropic core) reflected by the smectic-*A* layer structure with well-defined spacing [4–6]. Smectic-*A* straight filaments elongate when liquid crystal (LC) materials are cooled from an isotropic phase. Upon further cooling, these straight filaments become unstable and buckle continuously [4–6]. We note that the buckled filaments grow at constant periodicity (Fig. 1), and the periodically buckled filaments retain their shapes at a constant temperature.

Such a buckling phenomenon is similar to the buckling of elastic columns known in classical mechanics [9]. A column subjected to compression undergoes displacements transverse to the load when the increasing load reaches the critical buckling load (the Euler load) [9]. Recently, layer buckling in bulk smectic-*A* LC has been reported [10,11]. However, the periodic buckling of smectic-*A* filaments reported in this paper is apparently different from the layer buckling in bulk smectic-*A* LC. In addition, no theoretical studies have been made on the growth of smectic-*A* filaments from the viewpoint of the buckling of elastic tubes.

In this paper, we study the periodic buckling of smectic-*A* filaments both experimentally and theoretically. We first describe observations of the pattern formation of periodic buckling of smectic-*A* tubular filaments in an isotropic phase. Second, we describe the curvature elastic energy of the smectic-*A* filament. We then derive the shape equations for the smectic-*A* filament from the minimization of the curvature elastic energy with the periodic boundary condition. We find that an analytical solution to the shape equations well describes shapes of the periodically buckled filaments observed in the experiments. The dependence of the load on the length of the filament is numerically calculated based on the principle of virtual work using the analytical solution, and found to decrease with the lateral displacement of the buckled filament. We show that the critical buckling load is of the order of 1 pN.

II. EXPERIMENTAL SETUP AND RESULTS

Dodecyl alcohol (DODA) was mixed with octyloxycyanobiphenyl (8OCB) (a molar ratio of 8OCB to DODA is 4 to 6) to suppress a nematic phase and to observe a smectic-*A* phase in an isotropic phase [5]. Liquid crystal cells with dimensions of 10 mm$\times$10 mm$\times$100 μm were filled with the mixture. The LC cells were cooled at $\sim$0.05°C/min from the isotropic phase to the coexisting region of the smectic-*A* and isotropic phases to observe smectic-*A* filaments. The temperature of the LC cells was controlled in a

FIG. 1. Periodic buckling of a smectic-*A* filament observed at 41.0°C with polarizer and analyzer crossed. The cooling rate was −0.05°C/min. The bar indicates 50 μm.

*Electronic address: naito@pe.osakafu-u.ac.jp

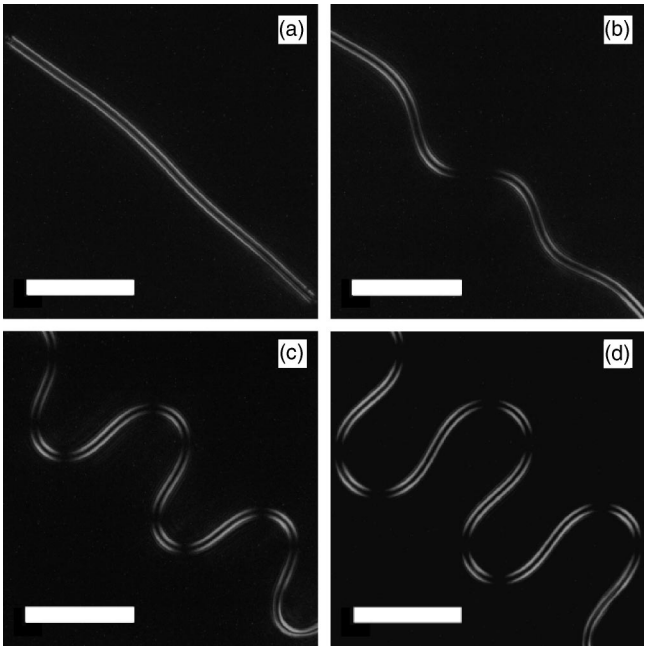

FIG. 2. Growth sequence of the smectic-*A* filament at −0.05°C/min observed with polarizer and analyzer crossed. Photographs (b), (c) and (d) show the same sample as in photograph (a) after 60, 120, and 150 s, respectively. Parenthesized figures correspond to lengths of the filaments per period. The bars indicate 50 μm. (a) 0 s(70.4 μm). (b) 60 s(78.4 μm). (c) 120 s(122.6 μm). (d) 150 s(178.0 μm).

hot stage (Instec HS1-i). The pattern formation of smectic-*A* filaments was observed with a polarizing microscope (Nikon X2TP-11) equipped with a CCD camera (Hitachi KP-F100).

A smectic-*A* phase initially appears in the form of spherical droplets at ~40°C when we cooled LC cells from an isotropic phase. These spherical droplets grow in size and then start elongating from the spherical droplets into straight filaments [Fig. 2(a)]. The filaments consist of concentric cylindrical smectic-*A* layers. The director of the smectic-*A* molecules is parallel to the layer normal [12]. Upon further cooling, the straight filaments buckle continuously at a constant periodicity by elongation [Figs. 2(b)–2(d)]. The periodicity of the buckled filaments is determined by the cooling rate at the initial stage of the periodic buckling instability of the straight filaments [15]. To show the metastability of the buckled filaments, we observe the filaments in cooling and heating cycles at ~0.01°C/min and at a constant temperature. Once the periodicity appears, the buckling process is found to be reversible with temperature, and these filaments retain their shape and position at a constant temperature. These results reveal that on cooling the buckled filaments are regarded as being in quasiequilibrium (mechanical equilibrium [13]) at each moment but not in thermal equilibrium.

III. THEORY

In this section, we solve the curvature elastic energy minimization problem for smectic-*A* filaments to predict the shapes of the buckled filaments theoretically. For the description of quasiequilibrium shapes of the smectic-*A* phase in an isotropic phase, we have proposed the free energy of the smectic-*A* phase consisting of the bulk energy (the Gibbs free energy differences between the isotropic and the smectic-*A* phases, and the curvature elastic energy of the smectic-*A* phase) and the interfacial energy (the surface energy of isotropic-smectic-*A* interface) [3,6]. In this paper, we deal with the time evolution of the smectic-*A* buckled filaments instead of thermal equilibrium shapes of the smectic-*A* phase. To do this, we assume that the filaments have a tubular structure with a thickness of $\rho_o - \rho_i$, where ρ_o and ρ_i are the outer and inner radii of the tube, respectively, since the existence of the inner isotropic core in smectic-*A* filaments has been reported in Ref. [5]. We then treat the periodicity of the buckled filaments and the values of ρ_o and ρ_i as being constant based on the experimental results, where ρ_o and ρ_i are determined as a function of the Gibbs free energy differences at the initial stage of the growth of the filaments [5,6]. In addition, we regard the buckling filaments, where lengths of the filaments change with time, as in quasiequilibrium at each moment of the growth process (in the calculation we treat the values of the lengths of the filaments as being constant). Therefore, we do not need to take into account the Gibbs free energy differences and the interfacial energy, and solve the curvature elastic energy minimization problem with those constant values of the buckled filaments measured from the experiment.

We first describe the general form of the curvature elastic energy of a smectic-*A* filament in an isotropic phase to derive the shape equations for the buckled filament. The curvature elastic energy of the smectic-*A* filament (F_C) is given by [6]

$$F_C = k_c \int_C \kappa(s)^2 ds + k_s \int_C ds, \tag{1}$$

where $k_c = \pi k_{11}(\rho_o^2 - \rho_i^2)/4$, k_{11} is the splay elastic constant, $\kappa(s)$ is the curvature defined along $\boldsymbol{r}(s)$, $\boldsymbol{r}(s)$ is the axial curve of the filament, and $k_s = \pi k_{11} \ln(\rho_o/\rho_i)$. Equation (1) is valid under the condition $\|\dot{\boldsymbol{r}}(s)\| = 1$, where $\dot{\boldsymbol{r}} = d\boldsymbol{r}/ds$ [in this case, s is defined as the arc length measured from a fixed point on $\boldsymbol{r}(s)$]. In order to derive the first variation of F_C using a variational method, we regard s as $s(u)$, and express F_C and $\boldsymbol{r}(s)$ as a function of u. Since u is an arbitrary variable ($\|\boldsymbol{r}(u)/du\| = 1$ is not satisfied), $F_C[\boldsymbol{r}(u)]$ is the general expression of Eq. (1). To do this, we replace ds with $\sqrt{\boldsymbol{r}' \cdot \boldsymbol{r}'}du$, where $\boldsymbol{r}' = d\boldsymbol{r}/du$. $\kappa(s)$ is recalculated from the differentiation with respect to du as a function of u, and we obtain

$$\kappa(u)^2 = \left[\frac{1}{\sqrt{\boldsymbol{r}' \cdot \boldsymbol{r}'}} \frac{d}{du} \left\{ \frac{1}{\sqrt{\boldsymbol{r}' \cdot \boldsymbol{r}'}} \frac{d\boldsymbol{r}}{du} \right\} \right]^2 = \left\{ \frac{\boldsymbol{r}'' \cdot \boldsymbol{r}''}{(\boldsymbol{r}' \cdot \boldsymbol{r}')^2} - \frac{(\boldsymbol{r}'' \cdot \boldsymbol{r}')^2}{(\boldsymbol{r}' \cdot \boldsymbol{r}')^3} \right\}, \tag{2}$$

where $\boldsymbol{r}'' = d^2\boldsymbol{r}/du^2$. Therefore, the general expression of the curvature elastic energy of the filament $F_C[\boldsymbol{r}(u)]$, has the form

$$F_C[\boldsymbol{r}(u)] = \int_C k_c \left\{ \frac{\boldsymbol{r}'' \cdot \boldsymbol{r}''}{(\boldsymbol{r}' \cdot \boldsymbol{r}')^2} - \frac{(\boldsymbol{r}'' \cdot \boldsymbol{r}')^2}{(\boldsymbol{r}' \cdot \boldsymbol{r}')^3} \right\} \sqrt{\boldsymbol{r}' \cdot \boldsymbol{r}'}\, du + k_s \int_C \sqrt{\boldsymbol{r}' \cdot \boldsymbol{r}'}\, du. \tag{3}$$

Next, we solve the minimization problem of $F_C[\boldsymbol{r}(u)]$ subjected to the constraint condition that the length of the filament is not changed (we regard the buckled filaments as in quasiequilibrium at each moment based on the experimental results). We define $F = F[\boldsymbol{r}(u)]$ as

$$F[\boldsymbol{r}(u)] = \int_C k_c \left\{ \frac{\boldsymbol{r}'' \cdot \boldsymbol{r}''}{(\boldsymbol{r}' \cdot \boldsymbol{r}')^2} - \frac{(\boldsymbol{r}'' \cdot \boldsymbol{r}')^2}{(\boldsymbol{r}' \cdot \boldsymbol{r}')^3} \right\} \sqrt{\boldsymbol{r}' \cdot \boldsymbol{r}'}\, du + \chi \int_C \{\sqrt{\boldsymbol{r}' \cdot \boldsymbol{r}'} - 1\} du, \tag{4}$$

where χ is the Lagrange multiplier. In Eq. (4), the second term of Eq. (3), which is proportional to the length of a filament, is disregarded because of the constraint condition. Let $\boldsymbol{r}(u)$ be the minimum solution of F at t, and we have the Taylor expansion of $F[\boldsymbol{r}(u) + \boldsymbol{\eta}(u)]$ about $\boldsymbol{r}(u)$,

$$F[\boldsymbol{r}(u) + \boldsymbol{\eta}(u)] = F[\boldsymbol{r}(u)] + \delta F + \delta^2 F + \delta^3 F + \cdots, \tag{5}$$

where $\boldsymbol{\eta}(u)$ is a perturbation on $\boldsymbol{r}(u)$ and a sufficiently small differentiable vector. δF is the first variation of $F[\boldsymbol{r}(u) + \boldsymbol{\eta}(u)]$, and is given by

$$\delta F = \int_C \left\{ \frac{\partial I}{\partial \boldsymbol{r}} \boldsymbol{\eta}^T + \frac{\partial I}{\partial \boldsymbol{r}'} \boldsymbol{\eta}'^T + \frac{\partial I}{\partial \boldsymbol{r}''} \boldsymbol{\eta}''^T \right\} du, \tag{6}$$

where

$$I = k_c \left\{ \frac{\boldsymbol{r}'' \cdot \boldsymbol{r}''}{(\boldsymbol{r}' \cdot \boldsymbol{r}')^2} - \frac{(\boldsymbol{r}'' \cdot \boldsymbol{r}')^2}{(\boldsymbol{r}' \cdot \boldsymbol{r}')^3} \right\} \sqrt{\boldsymbol{r}' \cdot \boldsymbol{r}'} + \chi(\sqrt{\boldsymbol{r}' \cdot \boldsymbol{r}'} - 1), \tag{7}$$

$\boldsymbol{\eta}' = d\boldsymbol{\eta}/du$, and $\boldsymbol{\eta}'' = d^2\boldsymbol{\eta}/du^2$. The condition necessary to minimize F_C subjected to the constraint condition is

$$\delta F = 0. \tag{8}$$

From Eqs. (6) and (8), we have

$$\int_C \left\{ \frac{\partial I}{\partial \boldsymbol{r}} \boldsymbol{\eta}^T + \frac{\partial I}{\partial \boldsymbol{r}'} \boldsymbol{\eta}'^T + \frac{\partial I}{\partial \boldsymbol{r}''} \boldsymbol{\eta}''^T \right\} du = 0. \tag{9}$$

δF is also expressed as

$$\delta F = \left[\frac{\partial I}{\partial \boldsymbol{r}'} \boldsymbol{\eta}^T + \frac{\partial I}{\partial \boldsymbol{r}''} \boldsymbol{\eta}'^T - \frac{d}{du} \left\{ \frac{\partial I}{\partial \boldsymbol{r}''} \right\} \boldsymbol{\eta}^T \right]_0^u + \int_C \left\{ \frac{\partial I}{\partial \boldsymbol{r}} - \frac{d}{du} \left\{ \frac{\partial I}{\partial \boldsymbol{r}'} \right\} + \frac{d^2}{du^2} \left\{ \frac{\partial I}{\partial \boldsymbol{r}''} \right\} \right\} \boldsymbol{\eta}^T du. \tag{10}$$

It is reasonable to assume that $\boldsymbol{r}(u)$ and $\boldsymbol{\eta}(u)$ are periodic functions of u because in the experiment the straight filaments buckle continuously at a constant periodicity as they grow (Fig. 2). Then, the first term of Eq. (10) vanishes. Thus, Eq. (8) is rewritten as

$$\frac{\partial I}{\partial \boldsymbol{r}} - \frac{d}{du} \left\{ \frac{\partial I}{\partial \boldsymbol{r}'} \right\} + \frac{d^2}{du^2} \left\{ \frac{\partial I}{\partial \boldsymbol{r}''} \right\} = 0. \tag{11}$$

Equation (11) is the Euler-Lagrange equation for F. We substitute I [Eq. (7)] into Eq. (11). Each term of Eq. (11) is calculated as follows:

$$\frac{\partial I}{\partial \boldsymbol{r}} = 0, \tag{12}$$

$$-\frac{d}{du} \left\{ \frac{\partial I}{\partial \boldsymbol{r}'} \right\} = k_c \left\{ \frac{2(\boldsymbol{r}'' \cdot \boldsymbol{r}')\boldsymbol{r}^{(3)}}{(\boldsymbol{r}' \cdot \boldsymbol{r}')^{5/2}} + \frac{2(\boldsymbol{r}^{(3)} \cdot \boldsymbol{r}')\boldsymbol{r}''}{(\boldsymbol{r}' \cdot \boldsymbol{r}')^{5/2}} + \frac{5(\boldsymbol{r}'' \cdot \boldsymbol{r}'')\boldsymbol{r}''}{(\boldsymbol{r}' \cdot \boldsymbol{r}')^{5/2}} + \frac{6(\boldsymbol{r}^{(3)} \cdot \boldsymbol{r}'')\boldsymbol{r}'}{(\boldsymbol{r}' \cdot \boldsymbol{r}')^{5/2}} - \frac{10(\boldsymbol{r}'' \cdot \boldsymbol{r}')(\boldsymbol{r}^{(3)} \cdot \boldsymbol{r}')\boldsymbol{r}'}{(\boldsymbol{r}' \cdot \boldsymbol{r}')^{7/2}} - \frac{15(\boldsymbol{r}'' \cdot \boldsymbol{r}')^2 \boldsymbol{r}''}{(\boldsymbol{r}' \cdot \boldsymbol{r}')^{7/2}} - \frac{25(\boldsymbol{r}'' \cdot \boldsymbol{r}')(\boldsymbol{r}'' \cdot \boldsymbol{r}'')\boldsymbol{r}'}{(\boldsymbol{r}' \cdot \boldsymbol{r}')^{7/2}} + \frac{35(\boldsymbol{r}'' \cdot \boldsymbol{r}')^3 \boldsymbol{r}'}{(\boldsymbol{r}' \cdot \boldsymbol{r}')^{9/2}} \right\} - \chi \left\{ \frac{\boldsymbol{r}''}{(\boldsymbol{r}' \cdot \boldsymbol{r}')^{1/2}} - \frac{(\boldsymbol{r}'' \cdot \boldsymbol{r}')\boldsymbol{r}'}{(\boldsymbol{r}' \cdot \boldsymbol{r}')^{3/2}} \right\}, \tag{13}$$

$$\frac{d^2}{du^2} \left\{ \frac{\partial I}{\partial \boldsymbol{r}''} \right\} = k_c \left\{ \frac{2\boldsymbol{r}^{(4)}}{(\boldsymbol{r}' \cdot \boldsymbol{r}')^{3/2}} - \frac{10(\boldsymbol{r}^{(3)} \cdot \boldsymbol{r}')\boldsymbol{r}''}{(\boldsymbol{r}' \cdot \boldsymbol{r}')^{5/2}} - \frac{10(\boldsymbol{r}'' \cdot \boldsymbol{r}'')\boldsymbol{r}''}{(\boldsymbol{r}' \cdot \boldsymbol{r}')^{5/2}} - \frac{2(\boldsymbol{r}^{(4)} \cdot \boldsymbol{r}')\boldsymbol{r}'}{(\boldsymbol{r}' \cdot \boldsymbol{r}')^{5/2}} - \frac{6(\boldsymbol{r}^{(3)} \cdot \boldsymbol{r}'')\boldsymbol{r}'}{(\boldsymbol{r}' \cdot \boldsymbol{r}')^{5/2}} - \frac{14(\boldsymbol{r}'' \cdot \boldsymbol{r}')\boldsymbol{r}^{(3)}}{(\boldsymbol{r}' \cdot \boldsymbol{r}')^{5/2}} + \frac{50(\boldsymbol{r}'' \cdot \boldsymbol{r}')^2 \boldsymbol{r}''}{(\boldsymbol{r}' \cdot \boldsymbol{r}')^{7/2}} + \frac{30(\boldsymbol{r}'' \cdot \boldsymbol{r}'')(\boldsymbol{r}'' \cdot \boldsymbol{r}')\boldsymbol{r}'}{(\boldsymbol{r}' \cdot \boldsymbol{r}')^{7/2}} + \frac{30(\boldsymbol{r}^{(3)} \cdot \boldsymbol{r}')(\boldsymbol{r}'' \cdot \boldsymbol{r}')\boldsymbol{r}'}{(\boldsymbol{r} \cdot \boldsymbol{r}')^{7/2}} - \frac{70(\boldsymbol{r}'' \cdot \boldsymbol{r}')^3 \boldsymbol{r}'}{(\boldsymbol{r}' \cdot \boldsymbol{r}')^{9/2}} \right\}. \tag{14}$$

$\boldsymbol{r}'$, $\boldsymbol{r}''$, $\boldsymbol{r}^{(3)} = d^3\boldsymbol{r}/du^3$ and $\boldsymbol{r}^{(4)} = d^4\boldsymbol{r}/du^4$ are, respectively, expressed as

$$\boldsymbol{r}' = \boldsymbol{t} \frac{ds}{du}, \tag{15}$$

$$\boldsymbol{r}'' = \kappa\, \boldsymbol{m} \left(\frac{ds}{du} \right)^2 + \boldsymbol{t} \frac{d^2 s}{du^2}, \tag{16}$$

$$\boldsymbol{r}^{(3)} = \{-\kappa^2\, \boldsymbol{t} + \dot{\kappa} \boldsymbol{m} - \kappa\tau\, \boldsymbol{b}\} \left(\frac{ds}{du} \right)^3 + 3\kappa\, \boldsymbol{m} \frac{d^2 s}{du^2} \frac{ds}{du} + \boldsymbol{t} \frac{d^3 s}{du^3} \tag{17}$$

and

$$\boldsymbol{r}^{(4)} = \{-3\kappa\dot{\kappa}\boldsymbol{t} + (-\kappa^3 + \ddot{\kappa} - \kappa\tau^2)\boldsymbol{m} + (-2\dot{\kappa}\tau - \kappa\dot{\tau})\boldsymbol{b}\} \left(\frac{ds}{du} \right)^4 + 6\{-\kappa^2\, \boldsymbol{t} + \dot{\kappa}\boldsymbol{m} - \kappa\tau\, \boldsymbol{b}\} \frac{d^2 s}{du^2} \left(\frac{ds}{du} \right)^2 + 3\kappa\, \boldsymbol{m} \left(\frac{d^2 s}{du^2} \right)^2 + 4\kappa\, \boldsymbol{m} \frac{d^3 s}{du^3} \frac{ds}{du} + \boldsymbol{t} \frac{d^4 s}{du^4}, \tag{18}$$

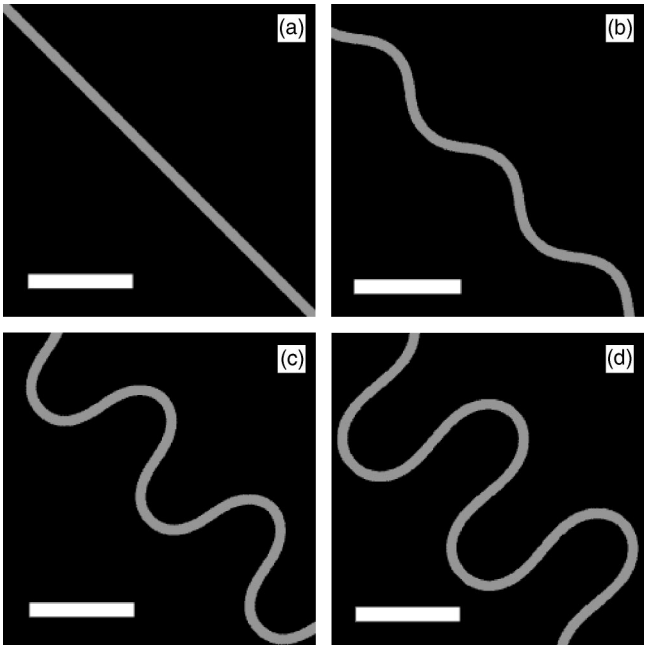

FIG. 3. Solutions to the shape equations for a buckled filament corresponding to the filaments shown in Fig. 2. The bars indicate 50 μm.

where $\boldsymbol{m}=\boldsymbol{m}(s)$, $\boldsymbol{b}=\boldsymbol{b}(s)$, and $\boldsymbol{t}=\boldsymbol{t}(s)$ are the normal, binormal, and tangential vectors of $\boldsymbol{r}(s)$, respectively, and $\dot{\kappa}$, $\ddot{\kappa}$, and $\dot{\tau}$ are $\dot{\kappa}=d\kappa/ds$, $\ddot{\kappa}=d^2\kappa/ds^2$, and $\dot{\tau}=d\tau/ds$, respectively. Substituting Eqs. (12)–(18) into Eq. (11), and disregarding the higher terms of ds/du (d^2s/du^2, d^3s/du^3, and d^4s/du^4), we obtain the shape equations

$$k_c(\kappa^3 - 2\kappa\tau^2 + 2\ddot{\kappa}) - \chi\kappa = 0, \tag{19}$$

$$2\dot{\kappa}\tau + \kappa\dot{\tau} = 0. \tag{20}$$

These are the shape equations for the buckled filament subjected to the constraint condition (the length of the filament is constant).

IV. DISCUSSION

We show an analytical solution to the shape equations [Eqs. (19) and (20)]. We define the tangential unit vector of $\boldsymbol{r}(s)$ to be

$$\boldsymbol{t}(s) = [\cos\,\phi(s), \sin\,\phi(s), 0]. \tag{21}$$

Inserting Eq. (21) into Eqs. (19) and (20) we have

$$\dot{\phi}^2 = \frac{\chi}{k_c} + \frac{f}{k_c}\cos[\phi(s) - \phi_0], \tag{22}$$

where f is a positive constant, ϕ_0 is an integration constant, and $\dot{\phi}=d\phi/ds$. Figure 3 shows the solutions to Eq. (22) with different values of f and χ. The values used in the calculation were $\rho_o=3.0$ μm, $\rho_i=0.7$ μm, $k_{11}=10$ pN [14], and $f=1.10$, 0.93, 0.46, and 0.25 pN and $\chi=-1.10$, -0.74, -0.09, and 0.02 pN for (a), (b), (c), and (d) in Fig. 3, respectively. f and χ are constants determined by the periodicity and the length of the buckled filaments. f corresponds to the load on the smectic-*A* filament, and the ratio of χ to f ranges from -1 to 1 and determines the shape of the buckled filament [7]. We see from Fig. 3 that the shapes obtained from the solutions to Eq. (22) are in quantitative agreement with the experimental results shown in Fig. 2. Therefore, it is shown that the periodically buckled filaments observed in the experiments are a form to minimize the curvature elastic energy of the smectic-*A* filaments under the constraint condition that the values of ρ_o and ρ_i, and the periodicity and the lengths of the buckled filaments are constant.

Equation (22) has a similar form to the solution derived by Zhou and Ou-Yang [7], which describes shapes of quench induced pattern formation of smectic-*A* filaments in an isotropic phase. In the initial stage of the growth of the smectic-*A* filaments at a rapid cooling rate of $>0.1\,^{\circ}\mathrm{C/min}$, the increase in the amplitude of buckling filaments along the growth direction is observed [6]. To explain the shapes of increasing amplitude of buckling filaments, they have assumed in Ref. [7] that the system is subjected to rapid cooling and no longer satisfies a quasiequilibrium condition, and that the value of k_{11} increases because of structural transition in the smectic-*A* filaments at the molecular level during the growth process, such as the *trans* to *cis* transition in alkyl chains of 8OCB molecules [6,7]. Using the solution derived by Zhou and Ou-Yang under the assumptions described above, they have been able to explain the shapes of the increasing amplitude of buckling filaments. They have concluded that the growth of the buckling filaments results from increasing curvature elastic energy converted from latent heat, and the increase in k_{11} causes the increase in amplitude of buckling filaments. Since we control LC cell temperature carefully at slow cooling rates of $<\sim 0.05\,^{\circ}\mathrm{C/min}$, we regard that the buckling filaments are in quasiequilibrium and that the value of k_{11} is a constant.

In bulk smectic-*A* LC, the layer buckling [10] is known as external (electric or magnetic) field-induced transition. The periodically buckled filaments shown here are apparently different from the field-induced transition. Layer buckling in the smectic-*A* phase induced by dilative strain has been reported [11], however, this layer buckling is also different from the buckling filaments because the buckling filaments consist of concentric tubes, whereas the bulk LCs consist of stacked planes of a smectic-*A* phase.

It is likely that the buckling of smectic-*A* filaments is a phenomenon similar to that of elastic columns known in classical mechanics; elastic columns undergo displacements when applied forces reach the critical buckling loads [9]. The differences between the buckling of the smectic-*A* filaments and that of elastic columns are the driving forces and the internal forces which occur when the bodies buckle. The driving forces for buckling of elastic columns are externally applied forces. Under the action of applied forces, the elastic columns change in shape and volume while keeping their masses, and extension and compression parts in the deformed columns cause internal forces. In case of the smectic-*A* filaments, the driving forces for buckling originate in the elongation (growth) of the filaments (this is the origin of the loads on the smectic-*A* filaments), and the changes in mass as

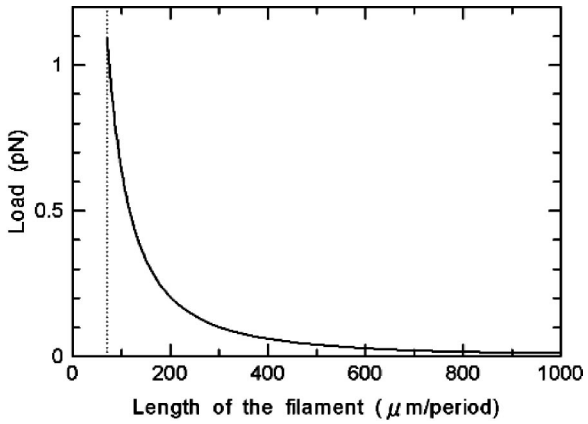

FIG. 4. The dependence of the load on the length of the filament per period (the periodicity of the buckled filament is 70 μm). The load decreases with increasing length of the filament.

well as in shape and volume take place when the bodies buckle. In addition, the buckling causes no extension or compression parts of the smectic-*A* filaments since the filaments consist of smectic-*A* layers that are regarded as two-dimensional liquids [14]. Only the internal forces caused by the splay deformation in smectic-*A* filaments occur in this case. During the growth of the buckled filaments, the forces caused by the splay deformation are balanced at each moment with the loads.

To understand the difference between the smectic-*A* filaments and the elastic columns, we numerically calculate the dependence of the load on the length of the filament [the lateral displacement (amplitude) of the buckled filament grows with the length of the filament] based on the principle of virtual work using Eqs. (3) and (22). We see from Fig. 4 that the critical buckling load of the filament is of the order of 1 pN and the load decreases with the length of the filament. It should be noted that the load of buckled elastic columns increases with the lateral displacement since the elastic columns buckle while keeping the mass constant. Zhou and Ou-Yang have estimated the average forces associated with the growth process of the buckled filaments to be of the order of 0.1 pN [7] (they use different assumptions from ours and have not mentioned the critical buckling forces), which is consistent with the values corresponding to the lengths in the 250 to 500 μm range shown in Fig. 4. It is interesting to note that the forces related to polymeric strings are often of the order of 10^{-2} to 10 pN [16,17].

V. CONCLUSIONS

We have studied the periodic buckling of smectic-*A* filaments both experimentally and theoretically. We have described the curvature elastic energy of the smectic-*A* filament by taking into account the internal forces caused by the splay deformation in smectic-*A* filaments. Then, we have derived the shape equations of the smectic-*A* filament with the periodic boundary condition from the minimization of the curvature elastic energy with the periodic boundary condition. It has been found that an analytical solution to the shape equations well describes shapes of the periodically buckled filament observed in the experiments. The buckling of smectic-*A* filaments is different from the layer buckling in bulk smectic-*A* LC in the sense that the smectic-*A* filaments in an isotropic phase have a cylindrical structure, and the filaments buckle not because of external-field application but because of forces originating in the elongation of the filaments. It is likely that the buckling of the filaments is a phenomenon similar to that of elastic columns described in classical mechanics.

The dependence of the load on the length of the filament has been numerically calculated based on the principle of virtual work. We have found that the critical buckling load is of the order of 1 pN and the load decreases with the lateral displacement (amplitude) of the buckled filament. The dependence of the load is contrary to that for elastic columns, where the load of a buckled elastic column increases with the lateral displacement. This is because the elastic column buckles while keeping the mass constant, whereas the smectic-*A* filament buckles with an increase in length, and the buckling of the smectic-*A* filament causes no extension or compression parts of the filament.

ACKNOWLEDGMENTS

We would like to thank Professor Z. C. Ou-Yang of Institute of Theoretical Physics, Academia Sinica for critical reading of this manuscript, and Merck, Ltd., Japan for supplying LC materials. We would also like to acknowledge financial support through a Grant-in-Aid for Scientific Research (Grant No. 13875063) from the Japan Society for the Promotion of Science, the Iketani Science and Technology Foundation (Grant No. 0131029-A), and the Sumitomo Foundation.

[1] S. L. Arora, P. Palffy-Muhoray, R. A. Vora, D. J. David, and A. M. Dasgupta, Liq. Cryst. **5**, 133 (1989).
[2] A. Adamczyk, Mol. Cryst. Liq. Cryst. **170**, 53 (1989); Thin Solid Films **244**, 758 (1994).
[3] H. Naito, M. Okuda, and Z. C. Ou-Yang, Phys. Rev. Lett. **70**, 2912 (1993); Phys. Rev. E **52**, 2095 (1995).
[4] P. Palffy-Muhoray, B. Bergersen, H. Lin, R. B. Meyer, and Z. Rácz, in *Pattern Formation in Complex Dissipative Systems*, edited by S. Kai (World Scientific, Singapore, 1992), p. 504; W. E and P. Palffy-Muhoray, J. Nonlinear Sci. **9**, 417 (1999).
[5] R. Pratibha and N. V. Madhusudana, J. Phys. II **2**, 383 (1992).
[6] H. Naito, M. Okuda, and Z. C. Ou-Yang, Phys. Rev. E **55**, 1655 (1997).
[7] H. Zhou and Z. C. Ou-Yang, Phys. Rev. E **58**, 5909 (1998).
[8] H. Naito, M. Todorokihara, Y. Hirose, and Z. C. Ou-Yang, J. Phys. Soc. Jpn. **67**, 713 (1998).

[9] A. E. H. Love, *A Treatise on the Mathematical Theory of Elasticity* (Dover, New York, 1926).
[10] R. E. Geer, S. J. Singer, J. V. Selinger, B. R. Ratna, and R. Shashidhar, Phys. Rev. E **57**, 3059 (1998).
[11] S. J. Singer, Phys. Rev. E **48**, 2796 (1993).
[12] Polarizing-microscope images were simulated to determine both the structure of the smectic-*A* filaments and the orientation of the smectic-*A* director in the filaments by comparing the simulated images with the experimentally obtained images. The details will be described in a future work by the current authors.
[13] S. Faetti and V. Palleschi, J. Chem. Phys. **81**, 6254 (1984).
[14] P. G. de Gennes, *The Physics of Liquid Crystals* (Clarendon, Oxford, 1975).
[15] The details will be described in a future work by the current authors.
[16] S. B. Smith, L. Finzi, and C. Bustamante, Science **258**, 1122 (1992); C. Bustmante, J. Marko, E. Siggia, and S. Smith, *ibid.* **265**, 1599 (1994); E. W. Wong, P. E. Sheehan, and C. M. Lieber, *ibid.* **277**, 1971 (1997).
[17] M. Dogterom and B. Yurke, Science **278**, 856 (1997), and references therein.